Int. J. Nonlinear Anal. Appl. 13 (2022) No. 1, 2395-2409
ISSN: 2008-6822 (electronic)
http://dx.doi.org/10.22075/ijnaa.2022.5940

Comparative study of two cases of single-phase HCMLI using IPDPWM technique for standalone PV system

Massara Glaa Yahya[a,*], Mawadah Glaa Yahya[b,*]

[a]*Medical Instruments Technology Engineering Department, AL-Esraa University College, Baghdad, Iraq*
[b]*Computer technology engineering, Al Salam University College, Baghdad, Iraq*

(Communicated by Madjid Eshaghi Gordji)

Abstract

The main aim of the paper is to reduce the Total Harmonic Distortion of a 9-level Hybrid Cascaded Multilevel Inverter for a standalone Photovoltaic system operated at Maximum powerpoint. The maximum power point is tracked using perturb and observe (P&O) method, a boost converter is used to implement this process. The output power is calculated using a small perturbation in the terminal voltage. The comparison between two cases of hybrid cascaded multilevel inverter using Phase Disposition Pulse Width Modulation has been done. Total harmonic distortion is minimized when one bridge is run in square wave mode and the other bridges are operated in pulse width modulation mode, according to the results of this comparison. The value of THD for HMLI output voltage is equal to 12.85 percent when all bridges are operated in PWM mode, according to simulation results. Finally, the results of the computer simulations using the MATLAB software are presented and discussed, along with a comparison of pulse width modulation strategies.

Keywords: Hybrid Cascaded Multilevel Inverter, Phase Disposition Pulse Width Modulation, Photovoltaic system, Maximum Power Point Tracking, Perturb and observe method, Total Harmonic Distortion.

*Corresponding author
Email addresses: massra@esraa.edu.iq (Massara Glaa Yahya), mawadah.g.yahya@alsalam.edu.iq (Mawadah Glaa Yahya)

Received: September 2021 *Accepted:* November 2021

1. Introduction

People are more likely to use renewable electricity as the need for electrical energy increases. Photovoltaic energy is the most widely used green energy source. Photovoltaic is a component that generates electricity from sunlight. Several MPPT approaches have been used in PV systems with the intent of enhancing the performance of PV panels. These MPPT techniques are used to transfer maximum power from the PV source to the load [7].

These methods include the well-known perturb and observe (P&O) [1, 10] and the incremental conductance (IC) [21] algorithms that are the most used. They are easy to be implemented and they recognize intuitively. However, they suffer from oscillation around the MPP and they cannot handle the environmental changes.

Artificial intelligent methods, including the fuzzy logic (FL) [14, 26], artificial neural network (ANN) [11], particle swarm optimization (PSO) [5], are also considered to mitigate the drawbacks of the previous methods. They have better performance outcomes and tend to be extremely superior to MPP tracking because, regardless of the abrupt weather changes, they are able to achieve full power easily and without any oscillation around the MPP. However, most of these techniques are costly and complicated in the implementation.

A photovoltaic output voltage is a DC voltage. Because the electrical system is dominated by an electric load with an AC voltage source, DC voltage cannot be used directly. A DC to AC voltage converter is therefore required. An inverter is a device that converts DC to AC voltage by using a switch component's switching conditions. The inverter's output voltage still has poor voltage quality, as measured by THD (THD). The voltage source requires a filter to produce a sinusoidal wave with the lowest THD voltage [17].

Multilevel inverters have gained popularity in medium voltage and high power applications due to their various advantages over typical two level inverters, such as lower switching losses, less harmonic distortions, and greater fault tolerance. Multilevel inverters are classified as Diode Clamped, Flying Capacitor, and Cascaded H-bridge [15]. As the number of output levels increases, the switching losses of the classical multilevel inverter topologies increase. This is overcome using a hybrid cascaded multilevel inverter. In a multilevel inverter topology, the number of switching devices, total harmonic distortion, the number of output levels, and the number of sources are the elements that determine performance [25].

In [13], it is suggested to use a 4-level symmetrical sub module as a basic cell for creating multiple DC voltage levels. Instead of using sixteen switches and four DC supplies like the standard cascaded hybrid bridge multilevel inverter (CHBMLI), [2] uses a new Asymmetrical Cascaded Hybrid Bridge Multilevel Inverter (ACHB-MLI) to produce a nine-level output waveform with only cascaded H-bridge inverter topology is proposed with a decoupling control method to produce multilevel output and reduce switching losses with low computation effort [24].

The inverter is controlled via pulse width modulation (PWM). The most extensively utilized pulse width modulation algorithms are Space Vector Modulation (SVM) and Multicarrier Pulse Width Modulation (MCPWM). The main disadvantage of SVM is that the user must select the best switching sequences. Choosing switching states is a difficult problem to implement in practice [18].

MCPWM was designed to solve the drawbacks of SVM. Multi-carrier pulse width modulations can be classified in to Phase shifted multi-carrier modulation and Level shifted multi-carrier modulation, which are divided into three methods: Phase Disposition Method, Alternative phase opposite disposition Method, and Phase opposite disposition Method. Phase Disposition Method [12]. Multicarrier PWM Strategies for hybrid Symmetrical Multilevel Inverter with Reduced Switch Count is proposed [8]. A design of photovoltaic based multilevel inverter using level shift pulse width modulation strat-

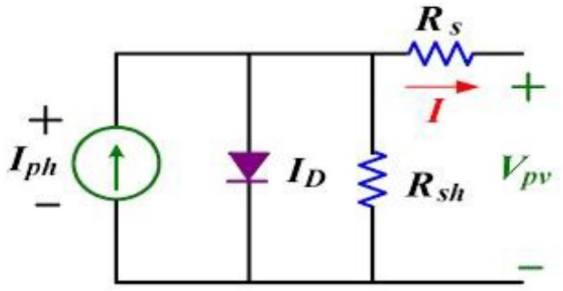

Figure 1: A PV cell's electrical equivalent circuit

egy is presented [12].
In this paper, the IPDPWM is applied to a 9-level single phase hybrid cascaded multilevel inverter in with each cell connected to a PV array and operating at maximum power point tracking (MPPT). A method that improved reduction in THD was presented, by operating one bridge in square wave mode and the remaining bridges in PDPWM mode.
This paper is organized as follows. The second section 2 presents the simulation of the photovoltaic system, while the third section 3 is presents the DC to DC converter. The sections 4, 5, and 6 are dedicated to HCMLI, IPDPWM, and THD, respectively. The sections 7 and 8 devoted to the investigation of the simulation results and the conclusion, respectively.

2. PV and MPPT simulation

Photovoltaic (PV) arrays transform solar energy into electrical energy in photovoltaic systems. PV arrays are widely used because they are clean, inexhaustible, and low-maintenance. Between the PV arrays and the load, photovoltaic systems require power converters. Equivalent circuit models define the I-V curve of a cell, module, or array as a continuous function. An example of a non-linear device is a photovoltaic cell connected in series with a diode (Fig. 1). During the night, the diode prevents reverse bias current from entering the panel [3].

When using the practical PV cell model, the shunt resistance is very large, while the series resistance is very small. As seen in the equation below, resistance values have little impact on overall cell performance [3].

$$l = I_{PV,cell} - I_o[exp(V + R_s I/V_t a) - 1] \tag{2.1}$$

$$V_t = N_s kT/q \tag{2.2}$$

Where,
I :the photovoltaic output current,
V :photovoltaic output voltage,
V_t :thermal voltage of array with Ns cells connected in series,
q :electron charge $(1.60217646e^{-19}C)$,
k :Boltzmann constant $(1.3806503e^{-23}JK^{-1})$.
T :temperature of the p-n junction in the unit of Kelvin,and
a :diode ideality constant.
In the following equation, $I_{PV,cell}$ represents the photovoltaic cell's light-generated current, which is proportional to solar irradiation and temperature:

$$I_{PV,cell} = (I_{PV,n} + K_i \Delta T)G/G_n \tag{2.3}$$

Table 1: The parameters of simulated PV module (Motech Americas IM72D3-330)

Model	**Clearline PV**
Maximum Power ($P_{\max}$)	330W
Current at Maximum Power (I_{mp})	8.76A
Voltage at Maximum Power (V_{mp})	37.66V
Open Circuit Voltage (V_{oc})	45.73V
Short Circuit Current (I_{sc})	9.27A
Number of cells (N)	72
Number of series cells N_s	2
Number of parallel cells N_p	1

$$\Delta T = T - T_n$$

Where,
$I_{PV,n}$: the light generated current at the nominal conditions of $25°C$ and $1000wm^{-2}$,
T: The actual temperature in unit Kelvin
T_n: The nominal temperature in unit Kelvin,
G: The solar irradiation by the PV surface is $G(wm^{-2})$,
G_n: the nominal solar irradiation is G_n.
The diode saturation current and its temperature dependence can be expressed as follows [6]:

$$I_o = [(I_{sc,n} + K_i\Delta T)/exp(V_{oc,n} + K_v\Delta T/aV_t) - 1] \tag{2.4}$$

Where,
I_o: diode saturation current,
K_v: open-circuit voltage/temperature coefficient,
K_i: short-circuit current/temperature coefficient,
$I_{sc,n}$: short-circuit current under the nominal condition, and
$V_{oc,n}$: open-circuit voltage under the nominal condition.
Parameters of simulated PV module (Motech Americas IM72D3-330) are summarized in Table 1.

The PV system should be operating at maximum power point. Because temperature and solar irradiation have an impact on the output power of a PV array; therefore, the maximum power point technique should be used when designing a photovoltaic device.
Various methods are used to track maximum power point. The most often utilized methods are:

1. Perturb and observe (hill climbing method) method
2. Incremental conductance method
3. Fractional open circuit voltage
4. Fractional short circuit current
5. Neural networks
6. Fuzzy logic

Perturb and observe (P&O) method is used in this paper due to its simplicity. A boost converter is used to implement this process. The boost converter is controlled by the algorithm presented in Fig.2 [4].

3. DC-DC Boost Converter

Fig. 3, illustrates the DC-DC boost converter. and the equation below shows how to calculate it:

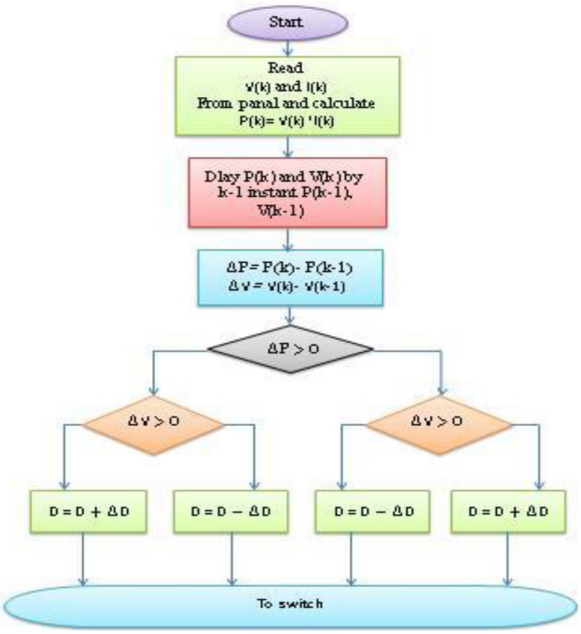

Figure 2: P and O MPPT algorithm flowchart

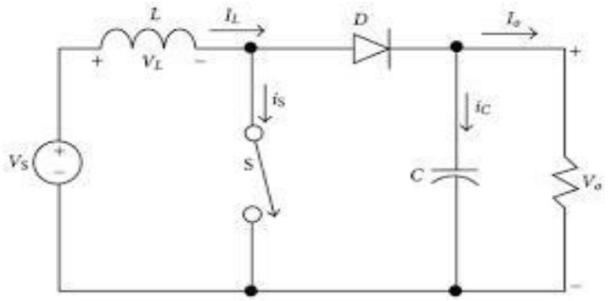

Figure 3: DC-DC boost converter

$$V_o = (1/1 - D)V_s \tag{3.1}$$

The boost converter is composed of a dc voltage source V_s, an inductor L (also known as a boost inductor), a filter capacitor C, a diode D, and a power semiconducting device as a switch S. The power is delivered to load resistance R at a higher voltage than input voltage. The duty cycle of the switch may be changed to regulate or adjust the voltage. When the switch is closed, the boost converter operates in the charging mode, and when the switch is open, the boost converter operates in the discharging mode [9].

4. Hybrid Cascaded Multilevel Inverters

The literature discusses a variety of multilevel inverter topologies, including cascaded H-bridge, flying capacitors, and clamping diodes multilevel inverters. The CHMI has a number of advantages over the other two inverters discussed. Because it is not utilize flying capacitors or clamping diodes. The key disadvantage of CHMI is that it needs different DC sources, which results in high costs and switching losses.

Proposed Hybrid Multilevel Inverter HMI is derived from conventional CHMI. It consists of main

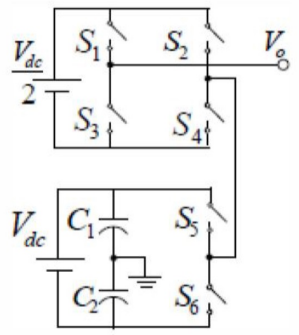

Figure 4: 5-level CHMI

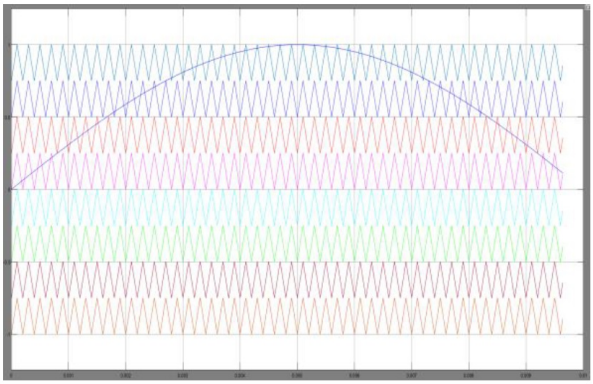

Figure 5: carrier signals in 9-level HCMLI

inverter and auxiliary inverters. These are cascaded to get the multilevel output. For 5-level main inverter consists of four switching devices cascaded to conventional H-bridge inverter, but the auxiliary inverter consists of two switching devices as show in Fig.4. The number of independent sources available for n level CHMI $(n-1)/2$ is $(n-1)$. In this study, the Simulink module of 9-level HMLI has been used, which necessitates the use of four independent sources. In general, renewable energy sources like same-rated solar panels, wind energy sources, or fuel cells can be employed as independent sources [25].

5. Phase Disposition SPWM (IPDSPWM) Switching Method

The amplitude and phase of different cell carrier waves that are compared to the desired sinusoidal wave are the same in this switching system, but the dc level of them differs. The amplitude of carrier waves in n-level CMLI is $2/(n-1)$. However, the number of carrier signals in n-level HCMLI is $n-1$ [19], in a 9-level CHB inverter, the amplitudes are 1/4 and number of carrier signals is 8 as shown in Fig.5.

6. Total Harmonic Distortion

Integer multiples of the fundamental frequency are harmonics in current and voltage. If the fundamental frequency is 60Hz, then the 2nd harmonic is 120Hz, the 3rd is 160Hz, etc. The Total Harmonic Distortion (THD) is the most important criterion for evaluating the quality of the voltage delivered by an inverter.

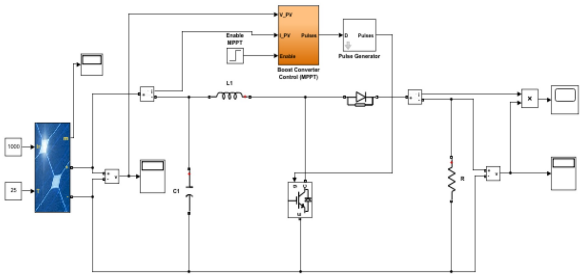

Figure 6: Single-phase PV and MPPT SIMULINK

THD is known as [16, 22, 23, 20], THD is a measure of the shape similarity between a waveform and its fundamental part.

$$THD = \sqrt{V_{o2}^2 + V_{o3}^2 + V_{o4}^2 + ... + V_{on}^2}/V_{o1} \tag{6.1}$$

Where V_{on} is the RMS output voltage of n^{th} harmonic and $n = 1$ is the fundamental frequency.

7. Simulation Results

In this section, the simulation of PV and MPPT algorithm is presented. Both the P-V and I-V characteristics of variable solar irradiation with constant model at temperature ($25°C$) and the Varying Temperature with Constant Solar Irradiance $1000W/m^2$ are verified. All simulation models are developed using MATLAB/SIMULINK.
The two cases of hybrid cascaded multilevel inverter using Phase Disposition Pulse Width Modulation has been done. They were supplied by a photovoltaic array that was set to maximum power point tracking. (MPPT). Fast Fourier Transformer (FFT) is used to calculate the harmonic spectrum of the output voltage of Hybrid Cascaded Multilevel Inverter (HCMLI). Additionally, the results of two cases are compared to verify the reduction in the value of THD for HMLI output voltage.

7.1. Simulation Results of PV Model and MPPT

The block diagram of the Simulink method for the PV array with MPPT connected to a DC/DC boost converter is shown in Fig.6. The output of the DC/DC converter is connected to an 80Ω load resistance.

The output current, voltage and power of each PV array for $1000W/m^2$ and $25°C$ are shown in Fig.7.

The output voltage, current, and power of DC/DC boost converter for $1000W/m^2$ and $25°C$ are shown in Fig.8.

A Motech Americas IM72D3-330 (two series modules and one parallel strings) solar PV model at two conditions were tested.
Fig.9 show the simulation results of the first condition of P-V, I-V features with variable solar irradiation ($100W/m^2, 500W/m^2$ *and* $1000W/m^2$) with fixed temperature in the simulation ($25°C$) respectively.
Solar cell I-V and P-V curves are highly reliant on solar irradiation values. It is obvious that as solar irradiation increases, the current generated increases, as does the maximum output power (Pm).

The simulation results of the second condition of P-V, I-V features with variable temperature from $25°C$ and $75°C$ and fixed solar irradiance $1000W/m^2$ are shown in Fig.10. In this condition, open circuit voltage (V_{OC}) and maximum power output of P-V model drop as cell temperature rises.

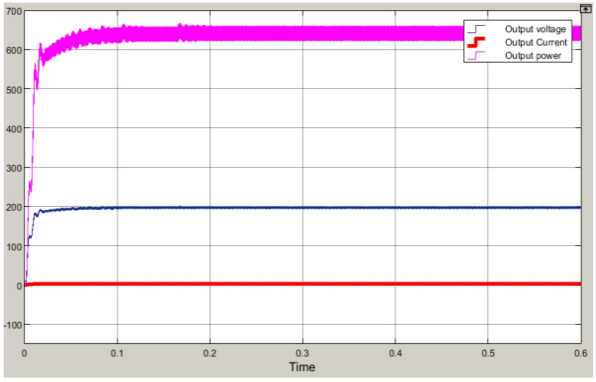

Figure 7: Output current, voltage and power of PV array for $1000W/m^2$ and $25°C$

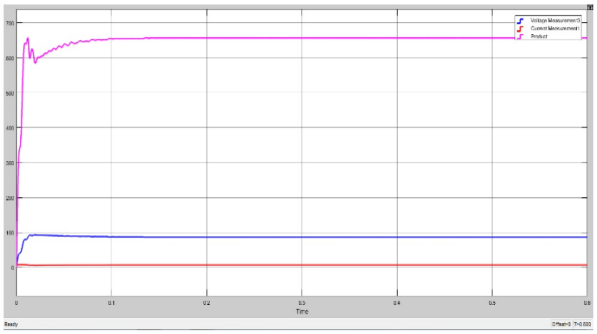

Figure 8: Output voltage, current, and power of DC/DC boost converter for $1000W/m^2$ and $25°C$

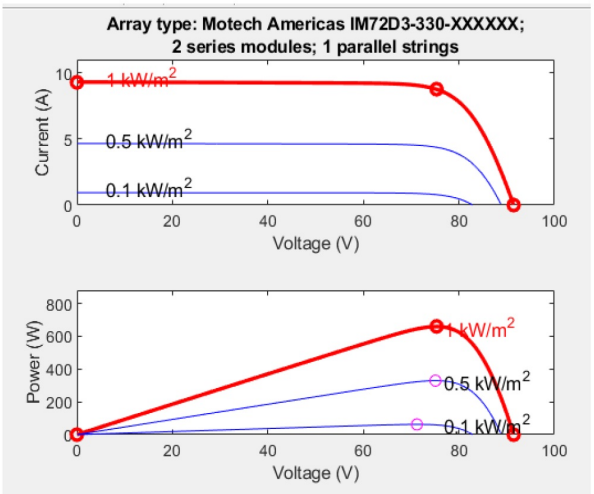

Figure 9: I-V and P-V curves of Motech Americas IM72D3-330 a solar cell with constant model temperature

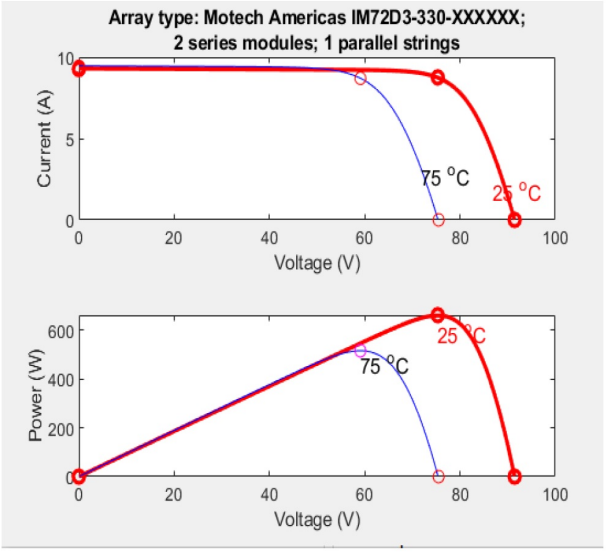

Figure 10: I-V and P-V curves of Motech Americas IM72D3-330 a solar cell with constant solar irradiance

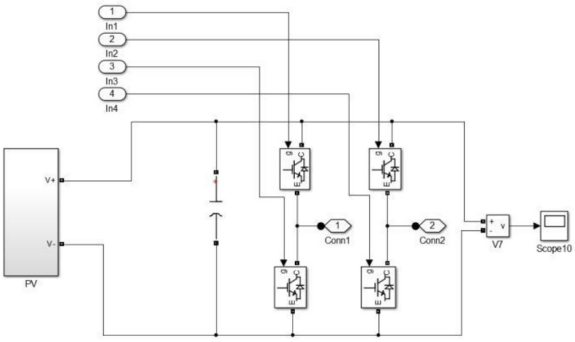

Figure 11: Simulink module of the cell of main inverter for HCMLI

7.2. Simulation Results for Single Phase 9-level HCMLI with Operating All Bridges in PWM Mode

An IPDPWM 9-level single-phase HCMLI has been simulated for a modulation index switching frequency is 5kHz and the carrier frequency is 50Hz.

PV array-fed multilevel inverter operating at maximum power point. The 9-level HCMLI has three cells main inverter and one cell auxiliary inverter, the main inverter has four switching devices (IGBT's) and four antiparallel diodes to feed back the energy to the dc source, but the auxiliary inverter has only two switching devices (IGBT's) and two antiparallel diodes as shown in Fig.11 and Fig.12, respectively.

An IPDPWM 9-level single-phase HCMLI with RL load ($R = 100\Omega$ *and* $L = 0.5H$) is shown in Fig.13.

As shown in Fig.14, the carrier waves of a 9-level HMLI with a switching frequency of 5kH are compared to a desire reference sinusoid wave.

Fig.15 shows the output current and voltage of an HCMLI inverter using the IPDPWM technique.

Fig.16 shows an FFT study of the output voltage of a single phase 9-level hybrid cascaded multilevel inverter using IPDPWM.

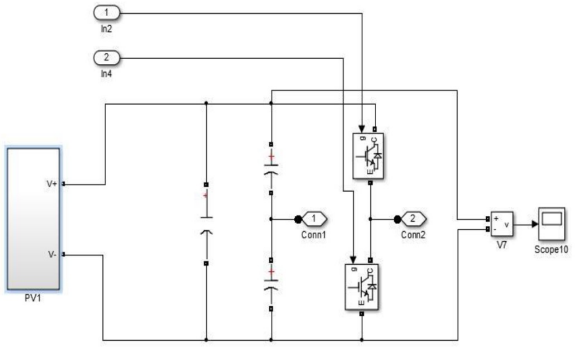

Figure 12: Simulink module of the cell of auxiliary inverter for HCMLI

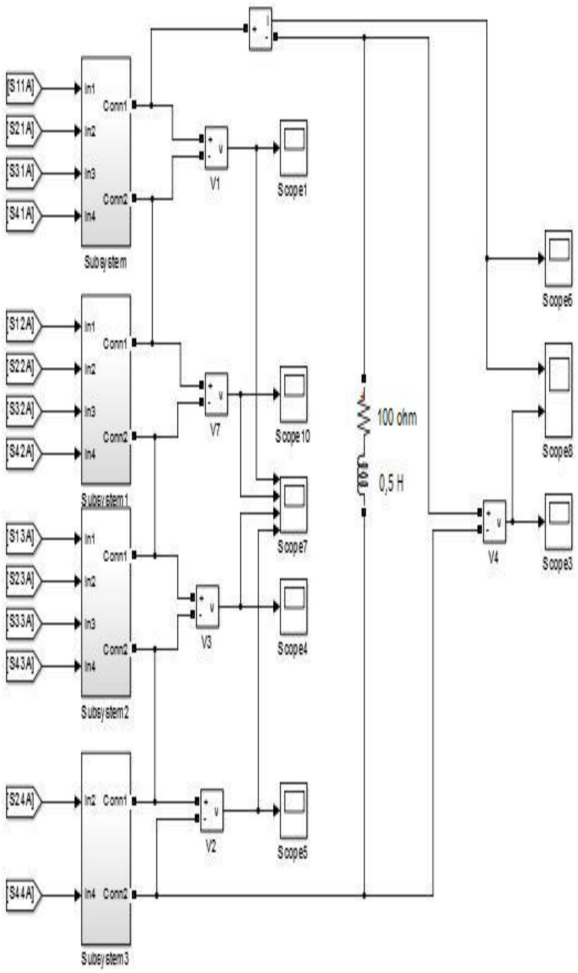

Figure 13: 9-level single phase hybrid multilevel inverter

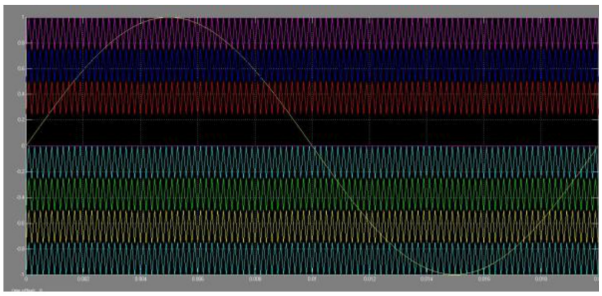

Figure 14: Comparison between the carrier waves and reference sinusoidal wave for 9-level HMLI

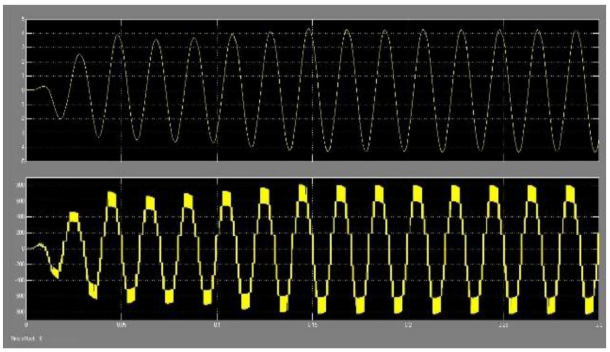

Figure 15: Output current and voltage of HCMLI inverter by applying IPDPWM technique

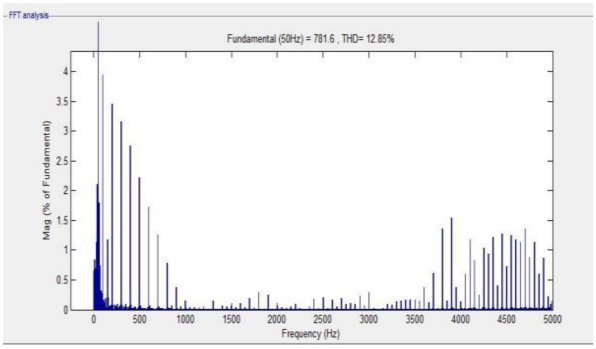

Figure 16: FFT analysis of output voltage

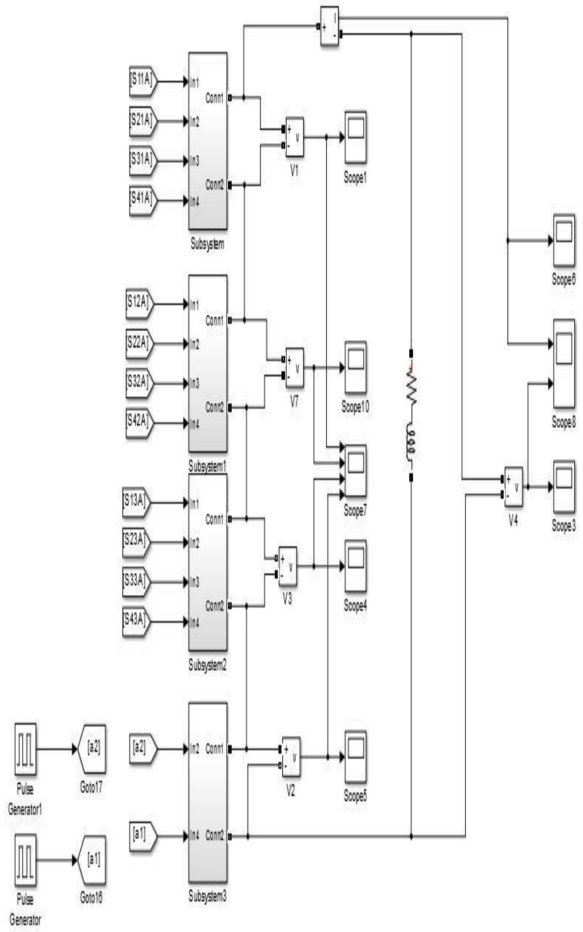

Figure 17: IPDPWM nine-level single phase HCMLI technique

Table 2: Analysis of THD and peak voltage of fundamental for different operating case of hybrid cascaded inverter

	THD	**Peak(V)**
HMLI for case1	12.85%	781.6
HMLI case2	11.34%	801.8

7.3. Simulation Modules for Single Phase 9-Level HCMLI When Square Wave Mode Was Used for One Bridge and the Remaining Bridges are Operated in Pulse Width Modulation

Fig.17. shows a Simulink module for a 9-level single phase HCMLI when square wave mode was used for one bridge and the remaining bridges are operated in pulse width modulation operates.

As shown in Fig. 18, the carrier waves of a 9-level HMLI with a switching frequency of 5kH are compared to a desire reference sinusoid wave.

Fig. 19 shows the output current and voltage of an HCMLI inverter when square wave mode was used for one bridge and the remaining bridges are operated in pulse width modulation (PWM).

Fig. 20 shows the FFT analysis of the output voltage of a single phase 9-level hybrid cascaded multilevel inverter when square wave mode was used for one bridge and the remaining bridges are operated in pulse width.

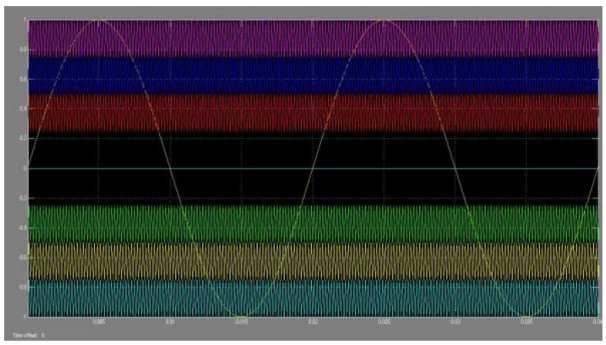

Figure 18: IPDPWM carrier and reference signals for HCMLI

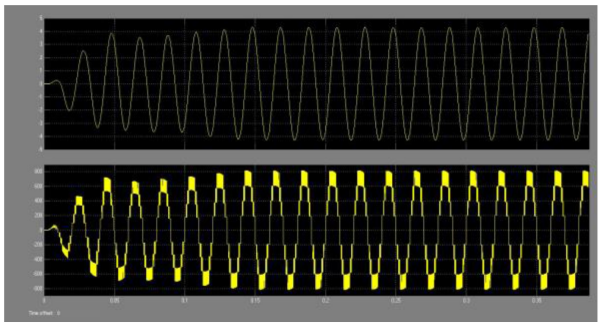

Figure 19: Output current and voltage of HCMLI

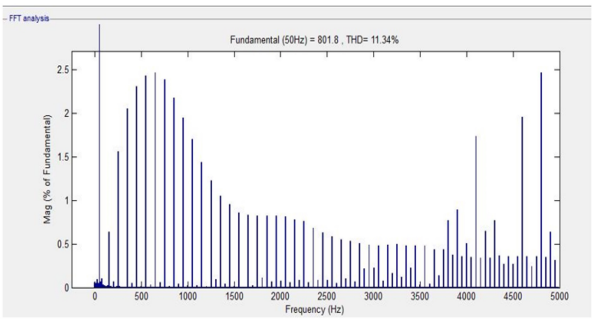

Figure 20: FFT analysis of output voltage

8. Conclusion

The two cases of HCMLI switching methods for standalone solar energy applications are presented in this paper. The square wave mode was used with the IPDPWM switching method to reduce THD in the HCMLI. This approach was used on a 9-level HMLI that was fed by PV arrays and run at MPPT. The value of THD for HMLI output voltage is equal to 12.85 percent when all bridges are operated in PWM mode, and the value of THD for HMLI output voltage is equal to 11.34 percent when square wave mode was used for one bridge and the remaining bridges are operated in pulse width modulation. According to simulation results, the reduction in THD is equal to 1.51%.

References

[1] M. Abdel-Salam, M.T. El-Mohandes and M. El-Ghazaly, *An efficient tracking of MPP in PV systems using a newly-formulated P & O MPPT method under varying irradiation levels*, J. Electr. Eng. Technol. 15(1) (2020) 501–513.

[2] Z.E. Abdulhamed, A.H. Esuri and N.A. Abodhir, *New topology of asymmetrical nine-level cascaded hybrid bridge multilevel inverter*, 2021 IEEE 1st Int. Maghreb Meet. Conf. Sci. Techniq. Automatic Control and Computer Engin. MI-STA, Tripoli-Libya, (2021) 430–434.

[3] C.C. Ahmed, M. Cherkaoui and M. Mokhlis, *PSO-SMC controller based GMPPT technique for photovoltaic panel under partial shading effect*, Int. J. Intell. Eng. Syst. 13(2) (2020) 307–316.

[4] K. Boudaraia, H. Mahmoudi and A. Abbou, *MPPT design using artificial neural network and backstepping sliding mode approach for photovoltaic system under various weather conditions*, Int. J. Intell. Eng. Syst. 12(6) (2019) 177–186.

[5] F.M. De Oliveira, S.A.O. Da Silva, F.R. Durand, L.P. Sampaio, V.D. Bacon and L.B.G. Campanhol, *Grid-tied photovoltaic system based on PSO MPPT technique with active power line conditioning*, IET 9(6) (2016) 1180–1191.

[6] R. El Idrissi, A. Abbou and M. Mokhlis, *Backstepping integral sliding mode control method for maximum power point tracking for optimization of PV system operation based on high-gain observer*, Int. J. Intell. Eng. Syst. 13(5) (2020) 133–144.

[7] R. El Idrissi1, A. Abbou, M. Mokhlis and M. Salimi, *Adaptive backstepping controller design based MPPT of the single-phase grid connected PV system*, Int. J. Intell. Eng. Sys. 14(3) (2021) 282–293.

[8] U. Gajula and G. Eragamreddy, *Multicarrier PWM strategies for hybrid symmetrical multilevel inverter with reduced switch count*, Int. J. Eng. Advanced Tech. 9 (2020) 860–866.

[9] T.W. Hariyadi and A. Adriansyah, *Comparison of DC-DC converters boost type in optimizing the use of solar panels*, 2nd Int. Conf. Broadband Commun. Wireless Sensors and Powering (BCWSP), Yogyakarta, Indonesia, (2020) 189–194.

[10] A. Harrag and S. Messalti, *PSO-based SMC variable step size P & O MPPT controller for PV systems under fast changing atmospheric conditions*, Int. J. Numer. Model. Electron. Networks, Devices Fields 32(5) (2019).

[11] L.P.N. Jyothy and M.R. Sindhu, *An artificial neural network based MPPT algorithm for solar PV system*, In: Proc. Of the 4th International Conference on Electrical Energy Systems, ICEES 2018, (2018) 375–380.

[12] O. Kumar, M. Goyal and R. Mishra, *Modified PV based hybrid multilevel inverters using multicarrier PWM strategy*, Fourth Int. Conf. Elect. Commun. Aerospace Technol. (ICECA-2020), (2020) 460–464.

[13] S.S. Lee, M. Sidorov, C.S. Lim, N.R.N. Idris and Y.E. Heng, *Hybrid cascaded multilevel inverter (HCMLI) with improved symmetrical 4-level submodule*, IEEE Trans. Power Electron. 33(2) (2018) 932–935.

[14] X. Li, H. Wen, Y. Hu and L. Jiang, *A novel beta parameter based fuzzy-logic controller for photovoltaic MPPT application*, Renew. Energy 130 (2019) 416–427.

[15] P. Manoharan, S. Rameshkumar and S. Ravichandran, *Modelling and implementation of cascaded multilevel inverter as solar PV based micro inverter using FPGA*, Int. J. Intell. Eng. Syst. 11(2) (2018) 18–27.

[16] H.R. Muhammad, *Power Electronics: Circuits, Devices, and Applications*, Pearson/Prentice Hall, 2004.

[17] K.B. Nagasai and T.R. Jyothsna, *Harmonic analysis and application of PWM techniques for three phase inverter*, Int. Res. J. Eng. Tech. 03 (2016) 1228–1233.

[18] H.P. Nguyen, D.T. Nguyen and M.T. Chau, *Carrier-based PWM method for indirect matrix converters based on space vector analysis*, Int. J. Intell. Eng. Syst. 13(6) (2020) 307–317.

[19] R. Sarker, *Phase disposition PWM (PD-PWM) technique to minimize WTHD from a three-phase NPC multilevel voltage source inverter*, IEEE Int. Conf. Convergence Engin. (2020) 220–224.

[20] T.S. Sasank, P.R. Ganesh, N.P. Kumar, B. Jena and A.J. Obaid, *Cryogenic analysis of junctionless nanowire MOSFET during underlap in lower technology nodes*, J. Phys.: Conf. Ser. 1879 (2020).

[21] L. Shang, H. Guo and W. Zhu, *An improved MPPT control strategy based on incremental conductance algorithm*, Prot. Control Mod. Power Syst. 5(1) (2020).

[22] S. Sharma and A.J. Obaid, *Optimal design, simulation and implementation of solar photo-voltaic panels in hybrid electric vehicles using CATIA V5R19 software integrated with ANSYS 13.0 versions*, J. Phys.: Conf. Ser. 1530(1) (2020).

[23] H. Singh, J. Singh, S. Sharma, S.P. Dwivedi and A.J. Obaid, *Comparative performance of copper, graphite, brass and aluminium/graphite-based different tool electrodes for optimizing the material removal rate during die-sinking EDM of stir-casted, Al6061/SiC- MMCs for Sustainable Manufacturing and Energy Applications*, J. Green Engin. 11(1) (2021) 922–938.

[24] K. Tan, H. Wang and C. Wang, *A decoupling control method for hybrid cascaded H-bridge inverter*, IEEE 9th Int. Power Electronics and Motion Control Conf. (IPEMC2020-ECCE Asia), (2020) 2469–2471.

[25] M. Thirumalai and V. Prakash, *Design and implementation of hybrid multilevel inverter for high output efficiency*, Int. Conf. Smart Struct. Syst. (JCSSS-2013), Chennai, INDIA, (2013) 41–45.

[26] U. Yilmaz, A. Kircay and S. Borekci, *PV system fuzzy logic MPPT method and PI control as a charge controller*, Renewable and Sustainable Energy Rev. 81 (2018) 994–1001.